Supporting Information

Cho et al. 10.1073/pnas.1400113111

SI Materials and Methods

Animals and Social Defeat Model. All animal experiments were approved by the Walter Reed Army Institute of Research Institutional Animal Care and Use Committee, and research was conducted in a facility fully accredited by the Association for the Assessment and Accreditation of Laboratory Animal Care International. Mice were maintained in a temperature-controlled room (21°C + 2 °C) on a reverse 12/12-h light/dark cycle (lights off at 0600 h). Male SJL albino mice weighing from 30 to 35 g were used as aggressors and housed individually in polycarbonate cages (48 × 27 × 20 cm) for 1 mo, with food and water provided ad libitum. We used three different strains of mice as subjects: C57BL/6j, DBA/2j, and BALB/cj. The subject mice weighed 20–25 g and were housed individually for 1 wk before the initiation of experiments. The experimental animals were kept in a wire mesh box inside the aggressor's cage for 6 h/d for either 5 or 10 consecutive d. Animals were randomly assigned to an aggressor cage. Each subject mouse (intruder) was placed three to five times within the home cage of an aggressor mouse (resident) and received bites/attacks for up to 2 min [or until 10 attacks/bites occurred (whichever came first)]. Animal behavior was evaluated using the partition (barrier) test immediately after the last direct contact with the aggressor. Each day, the stress procedure occurred at different times, and a different resident mouse was used as the aggressor for each session. Body weight and temperature of the experimental mice were measured every day before the beginning of the social defeat period and on the return to their home cages. The interaction between the resident and the intruder was video-recorded. The cage was divided into three zones, and time spent in each zone was analyzed using a video-tracking tool (Ethovision; Noldus Information Technology). Control mice were kept inside of the wire mesh boxes inside of a large cage without any aggressor.

Pathological Evaluation. Briefly, heart samples were collected from the euthanized control and subservient mice and perfused in ice cold 4% (vol/vol) paraformaldehyde. Tissues were stained, sliced, and mounted, and a trained pathologist blinded to the animal condition identified and analyzed them using bright-field microscopy. Primary characteristics evaluated included arterial thrombus, myocardial degeneration and infiltration, lymphohistocytic epicarditis, myocarditis, and vasculitis. Each experimental batch consisted of five control and five subject mice. The most prominent changes observed in the heart tissues were vasculitis and myocarditis (Fig. S1), which are associated with heart diseases, such as cardiovascular disease and arthrosclerosis.

Tissue and RNA Isolation. Total RNA was isolated from individual mouse heart samples by homogenization in TRIzol reagent per the manufacturer's protocol (Life Technologies). The quality and quantity of the RNA samples were evaluated using a NanoDrop ND-1000 spectrophotometer (Thermo Scientific) and Agilent 2100 BioAnalyzer (Agilent).

Microarray Data Generation and Analysis. For each microarray experiment, 100 ng total RNA were reverse transcribed and followed by generation of cDNAs. The resulting cDNAs were transcribed and labeled with cyanine 3-CTP. The labeled antisense cRNAs were purified and hybridized to Agilent's 8 × 60,000 microarrays. The hybridization was carried out for 16 h at 45 °C. The arrays were washed and scanned using an Agilent scanner (Agilent). The scanned images of the arrays were converted and imported into the Institute for Systems Biology's Systems Biology Experiment Analysis Management System. As a preprocessing step, the sets of gene expression data in the same experimental group were merged together and then normalized using the quantile method.

For each experimental condition in study I and study II, the differentially expressed genes (DEGs) between stressed and control mice samples were identified using the moderated *t* test in R-package LIMMA (1). *P* values of genes were computed from the moderated *t* statistics, and the false discovery rate (FDR) was calculated using the Benjamini–Hochberg correction method (2). The set of DEGs was selected by considering the FDR (in this study, 0.1 was used as a cutoff value), fold changes (±1.5-fold was used for the experimental groups in study I and ±twofold was used for study II), and the absolute expression level (only genes with a mean expression level across samples greater than the overall mean expression were considered; i.e., so-called present genes). When multiple probes mapped to the same Entrez ID were identified as DEGs, only one probe with the maximum mean expression level was selected to make a unique set of DEGs. For study II [number of days of trauma exposure (T); number of days of rest after exposure (R); i.e., T1R1, T2R1, and T3R1 groups], 494 genes were chosen as DEGs, provided that they were showing an FDR less than 0.1 and fold changes between stressed and control samples greater than ±2 in at least one group.

microRNA (miRNA) expression profiling of the samples was performed using a two-channel Exiqon miRCURY LNA array, fifth generation (Exiqon). The labeling of samples and hybridization were carried out according to the manufacturer's instructions. The arrays were washed and scanned using an Agilent scanner, and then, the scanned images were processed using either Agilent Feature Extraction or Analyzer DG. For the preprocessing of two-channel microarray data, within-array normalization using LOWESS and between-array normalization using the quantile method were applied to the raw miRNA expression data of each experimental group. Because there are four identical replicated probes for each miRNA in the Exiqon microarray platform, they were consolidated by taking the median expression value over the replicated probes to remove redundancy.

Functional Enrichment Analysis. Functional enrichment to determine whether an input set of genes was overrepresented in a specific gene ontology (GO) term or known pathway was performed using the Fisher exact test. This test produced *P* values by computing the probability of observing a certain number of genes in the GO term or pathway by random chance. The Bonferroni method of multiplying *P* values by the total number of GO terms or known pathways tested was used for multiple testing corrections of functional enrichment.

For GO enrichment analysis, the gene annotation of *Mus musculus* was downloaded from the GO website (http://www.geneontology.org). For pathway enrichment analysis, all XML files storing pathway information were downloaded from the KEGG pathway website (http://www.genome.jp/kegg) and parsed for extracting the genes involved in each pathway.

Identification of Functional Modules. With a composite set of 713 DEGs identified from study I and study II, a semantic similarity-integrated modularization approach was used to identify functional gene modules. In this study, semantic similarity-integrated approach for modularization takes three 713 × 713 (symmetric) gene–gene pairwise similarity matrices for input. (*i*) The expression similarity matrix of each element (*i*th row and *j*th column: $1 \leq i$

and $j \leq 713$) was computed by taking the Pearson correlation between gene expression profiles of DEG i and DEG j. The composite profile, in which the expression profiles of T1R1, T2R1, T3R1, T5R1, and T10R1 groups were horizontally concatenated, was used to compute correlation. (*ii*) The topological similarity matrix of each element was obtained from the combined score between the pairs of DEGs. The combined score in the STRING 9.0 database represents the confidence of association between predicted/validated interacting proteins, and thus, it can be used as a similarity between (protein-coding) genes in a protein–protein interaction network (3). (*iii*) The semantic similarity matrix of each element represents the GO semantic similarity between the pair of genes. GO semantic similarity was calculated by the method by Wang et al. (4) using the same gene annotation used in functional enrichment analysis and the ontology information (OBO v1.2 format) downloaded from the GO website. Given three similarity measures, the combined similarity was calculated by converting individual similarity measures into probability values and then multiplying three probabilities to produce the joint probability.

Next, to find groups of DEGs with high expression and topological and semantic similarities, spectral clustering based on the Ng–Jordan–Weiss method was applied to the combined similarity matrix (5). The number of clusters was estimated by checking the elbow point in the plot of eigenvalues, and 23 gene modules were generated as a result.

Identification of Potential Regulators Responsible for Gene Modules. To find putative regulators that may control the gene modules identified, we adopted the enrichment analysis approach using the Fisher exact test, which could assess whether the DEGs in a certain module were overrepresented in a set of target genes of a certain regulator [transcription factor (TF) or miRNA].

The set of TF target information was obtained from four public databases. (*i*) Amadeus (http://acgt.cs.tau.ac.il/amadeus/download.html): metazoan compendium was downloaded, and mouse TF target information was extracted. Human TF target information was also used with the use of Mouse Genome Informatics (MGI) human–mouse orthology. (*ii*) TRED (http://rulai.cshl.edu/TRED): target information of 36 TF families was retrieved. MGI human–mouse orthology was used to convert data entries of humans. (*iii*) EdgeExpressDB (http://fantom.gsc.riken.jp/4/edgeexpress): a repository of predicted TF target information of humans assessed by deepCAGE. With MGI orthology, the human data entries were converted to mouse entries. (*iv*) MSigDB (http://www.broadinstitute.org/gsea/msigdb): C3 motif gene set (transcription factor targets) was retrieved and used. The set of miRNA target information was obtained from five public databases. (*i*) TargetScan Mouse 5.1 (http://www.targetscan.org): predicted/conserved targets of conserved miRNA families were used. (*ii*) PITA (http://genie.weizmann.ac.il/pubs/mir07/mir07_data.html): top predictions for mouse were used. (*iii*) miRTarget2 (http://mirdb.org/miRDB/): the predicted target list of miRDB v3.0 was used. (*iv*) microT (http://diana.cslab.ece.ntua.gr/microT/): microT v3.0 with loose threshold was used to retrieve the list of predicted targets of miRNAs. (*v*) miRanda-mirSVR (http://www.microrna.org/microrna/home.do): the predicted target list with good mirSVR score and conserved miRNA for mouse was used.

Between each module and each regulator in each database, the contingency table shown below could be formed, and the Fisher exact test of overrepresentation could be performed. FDR was calculated by the Bonferroni correction method.

	DEGs in the module	Total
Targets of a certain regulator stored in the database	m	n
Total	M	N

P value from the Fisher exact test is $P = 1 - \sum_{i=0}^{m-1} \frac{\binom{n}{i}\binom{N-n}{M-i}}{\binom{N}{M}}$. At the enrichment FDR less than 0.1, *E2f1*, *E2f2*, and miR-29b were significantly changed in our microarray datasets and chosen as relevant regulators for the corresponding modules.

Data Analysis of miR-29 Transfection. Using two-channel Agilent whole-mouse genome microarray 4 × 44,000, the gene expressions of a control sample and a treated sample collected 24 h after miR-29 transfection were profiled. Within-array normalization using LOWESS was performed in the Agilent Feature Extraction software to remove dye bias, and then, between-array normalization was done using the quantile method across all samples. In total, 2,530 genes were found to be significantly affected by miR-29 transfection (present and changes greater than ±1.5-fold). Comparing 2,530 genes with 713 posttraumatic stress disorder (PTSD) DEGs, 76 genes were inversely correlated between two datasets (most of them were up-regulated in the PTSD mouse model but down-regulated in response to miR-29 transfection). Although PTSD DEGs were not significantly overrepresented in the set of genes perturbed by miR-29 transfection (P value = 0.7745 calculated by the Fisher exact test), the genes overlapping in both sets of genes were strongly associated with the ECM remodeling processes.

Data Analysis of TGF-β Treatment to Human A549 Cell Lines (Epithelial-to-Mesenchymal Transition Model System). Using two-channel Agilent whole-human genome microarray 4 × 44,000, the gene expressions of the samples were profiled. Control and treated samples were collected 3, 5, 7, 9, 11, and 13 d after the TGF-β treatment (one sample at each time point in each condition). Preprocessing of the two-channel microarray data was done the same as described above. To identify temporally differentially expressed genes, the (log) fold changes between treated and control samples over time for each gene were obtained, and the area under the profile of fold changes was computed using the trapezoidal numerical integration approach along the time points. Note that the artificial fold change value of zero at time point 0 was added for the integration. Empirical null distribution of the area under the profile was obtained by 10,000 times permutation of sample labels. A P value for each gene was calculated by comparing the observed area with the empirical null distribution in a two-tailed manner, because down- and up-regulated genes would have negative and positive values of area under the profile, respectively. FDR was also computed using the Benjamini–Hochberg method. Through this approach, we identified 629 unique DEGs [epithelial-to-mesenchymal transition (EMT) DEGs] with FDR less than 0.1 and fold changes greater than two for at least one time point. Because the experiment was performed using human microarrays, MGI human–mouse orthology was used to convert human Entrez ID to mouse Entrez ID for comparison with the PTSD DEGs.

Comparing 629 EMT DEGs with 713 PTSD DEGs, 72 genes were shared in two sets of DEGs, and among them, 52 genes were either up- or down-regulated in both sets. The significance level (i.e., P value) of overrepresentation of PTSD DEGs in the set of EMT DEGs was 1.08×10^{-7} as calculated by the Fisher exact test (16,514 mouse orthologs of human genes in Agilent whole-human genome microarray 4 × 44,000 as total genes, 629 EMT DEG and 626 PTSD DEG orthologs of human, and 52 overlapped DEGs were used for the test).

1. Smyth GK, Michaud J, Scott HS (2005) Use of within-array replicate spots for assessing differential expression in microarray experiments. *Bioinformatics* 21(9):2067–2075.
2. Hochberg Y, Benjamini Y (1990) More powerful procedures for multiple significance testing. *Stat Med* 9(7):811–818.
3. Szklarczyk D, et al. (2011) The STRING database in 2011: Functional interaction networks of proteins, globally integrated and scored. *Nucleic Acids Res* 39(Database Issue):D561–D568.
4. Wang JZ, Du Z, Payattakool R, Yu PS, Chen CF (2007) A new method to measure the semantic similarity of GO terms. *Bioinformatics* 23(10):1274–1281.
5. Ng AY, Jordan MI, Weiss Y (2001) On spectral clustering: Analysis and an algorithm. *Advances in Neural Information Processing Systems* (MIT Press, Cambridge, MA), pp 849–856.

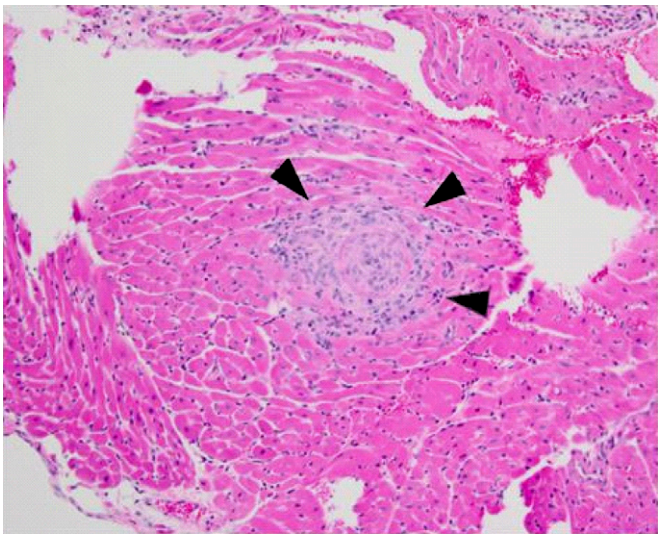

Fig. S1. Typical histopathology image of heart tissue. The myocardium and perivascular tissue are multifocally infiltrated with moderate numbers of lymphocytes and macrophages, with fewer plasma cells. The image (H&E, 10×) shows the lumen almost completely occluded, the wall thickened, and inflammatory cells expanding the vessel wall (arrowheads) and surrounding the vessel. Col, collagen.

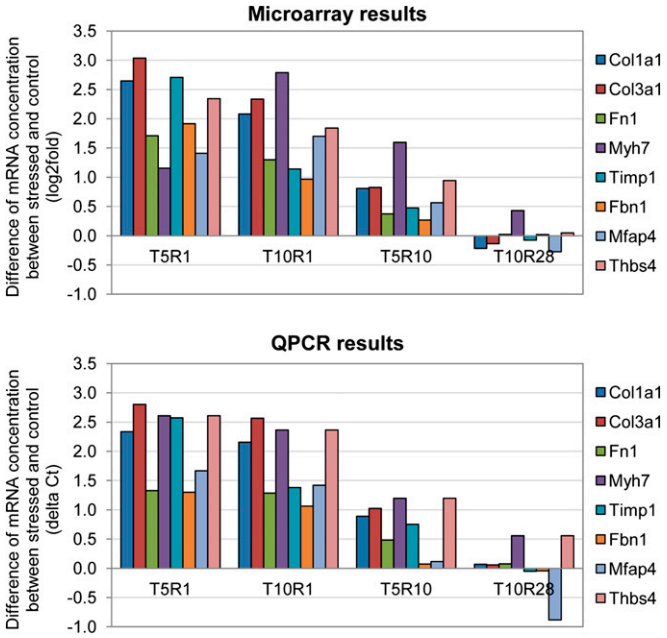

Fig. S2. Validation of gene expression changes observed in microarray experiments. The *y* axis represents the difference of mRNA concentration between stressed and control mice samples in log2 fold and ΔCt (threshold cycle) value in microarray and quantitative PCR (QPCR) results, respectively. The experimental group is indicated on the *x* axis.

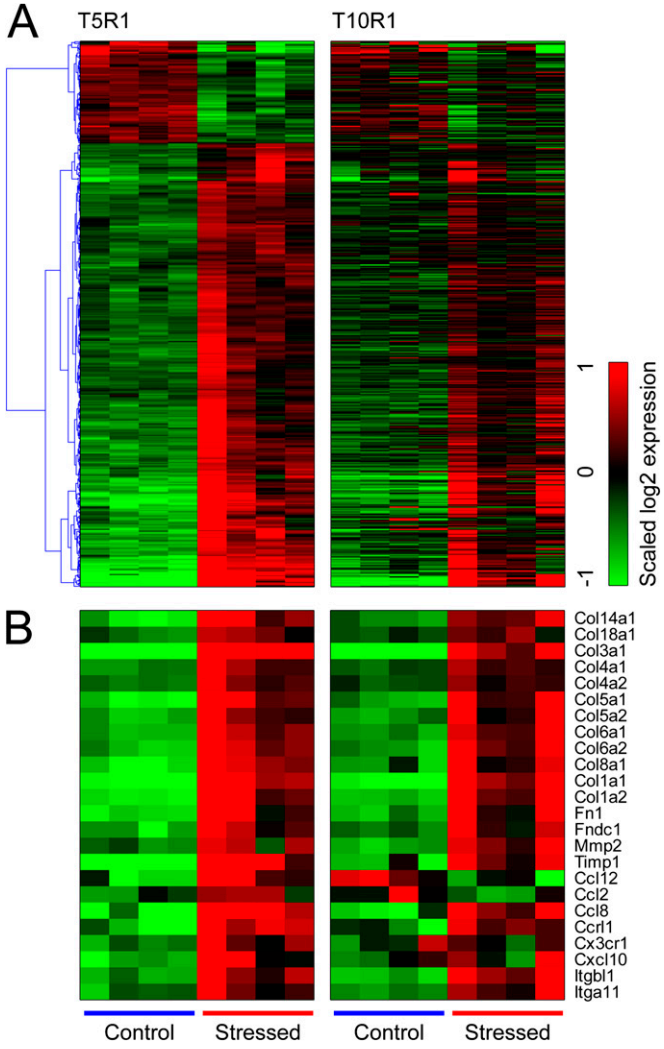

Fig. S3. (*A*) Heat map of 464 DEGs identified in either the T5R1 or T10R1 sample group. Among them, 455 DEGs were identified in T5R1, 40 DEGs were found in T10R1, and 31 DEGs were shared in both conditions. In each dataset, gene expression was scaled to have a zero mean and unit variance across samples. Red and green colors indicate higher and lower gene expression levels in the stressed mice samples, respectively. (*B*) Representative DEGs associated with extracellular remodeling processes and immune responses in T5R1 and T10R1 groups.

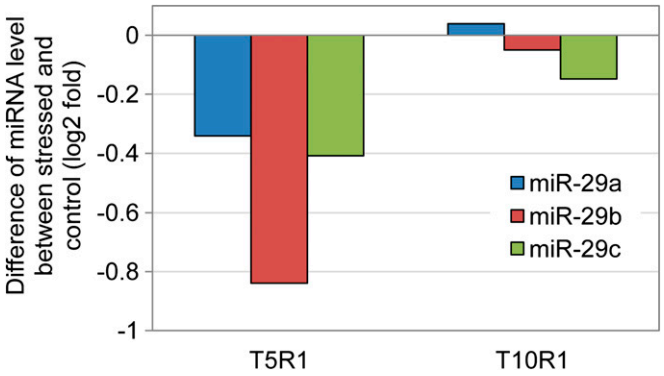

Fig. S4. The levels of miR-29 family members measured by microarray. The *y* axis represents the difference of miRNA concentration between stressed and control mice samples in log2 fold. The experimental group is indicated on the *x* axis.

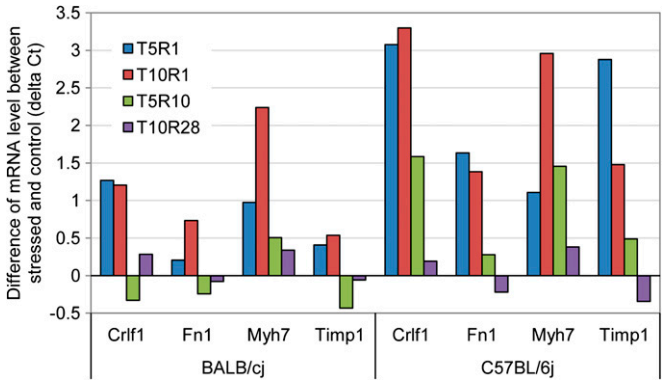

Fig. S5. QPCR validation of the expression changes of selected genes in BALB/cj and C57BL/6j mouse strains. The *y* axis represents the difference of miRNA concentration between stressed and control mice samples in ΔCt value. The gene symbols and mouse strains are indicated on the *x* axis.

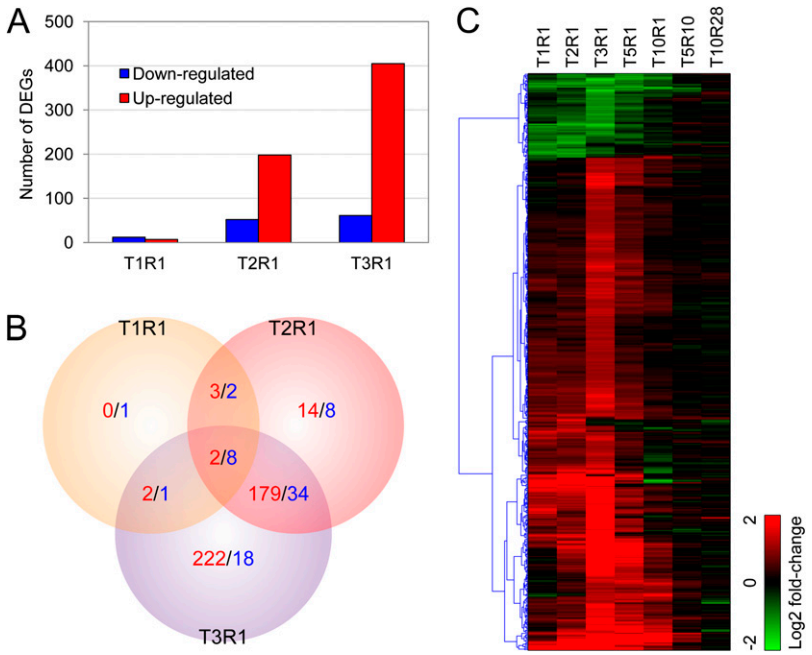

Fig. S6. (*A*) The number of DEGs identified from study II (T1R1, T2R1, and T3R1 groups). (*B*) Venn diagram of the total 494 DEGs identified in T1R1, T2R1, and T3R1 groups. Red and blue numbers represent the numbers of up- and down-regulated DEGs, respectively. (*C*) Heat map of 494 DEGs. Fold changes between stressed and control mice samples of the DEGs and the corresponding fold changes in T5R1, T10R1, T5R10, and T10R28 groups were concatenated, and then, hierarchical clustering was applied for visualization. The red and green colors represent the increased and decreased expression levels of the stressed samples compared with the control samples, respectively.

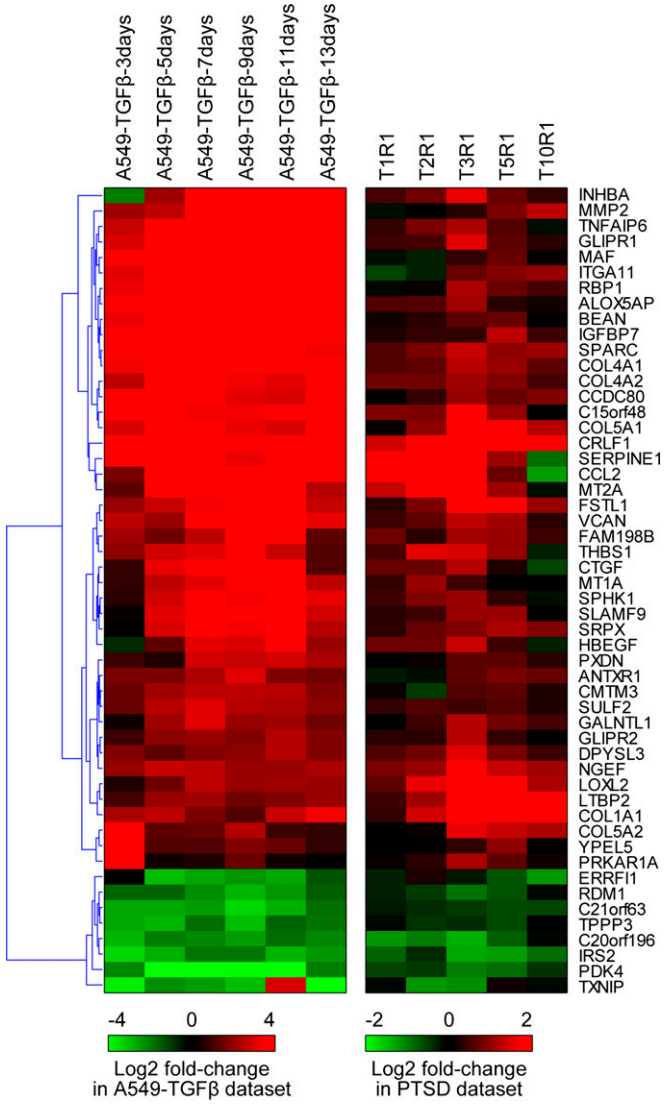

Fig. S7. Heat map of the subset of 713 DEGs (52 DEGs) that showed significant changes in the experiment of TGF-β treatment to A549 cell lines. Many collagen genes, such as Col1a1, Col4a1, Col4a2, Col5a1, and Col5a2, and EMT marker genes, including Mmp2 and connective tissue growth factor (Ctgf) are up-regulated in both PTSD and EMT model systems. It indicates that the EMT process might be involved in the repairing of heart tissues damaged by the social stress.

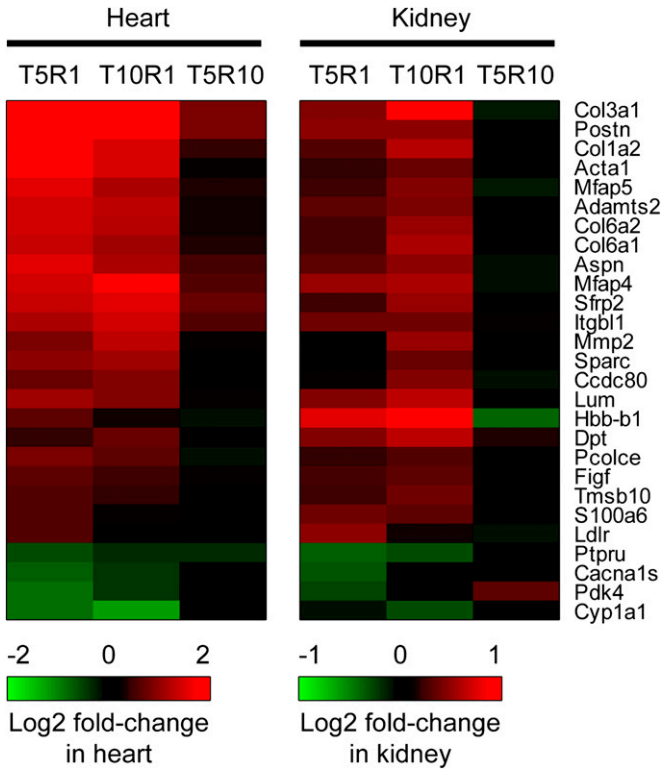

Fig. S8. Heat map of the selected genes that showed similar changes in heart and kidney samples of C57BL/6j mice. Genes with a correlation of fold changes in three groups (T5R1, T10R1, and T5R10) between heart and kidney that were greater than 0.7-fold (log2 scale) and genes with a fold change in the kidney greater than ±0.3 were chosen. Only very few genes were both highly correlated between heart and kidney and also significantly perturbed in the kidney. Several genes associated with ECM remodeling (Acta, Col1a2, Col3a1, Col6a1, Col6a2, Adamts2, Mfap4, Mfap5, Sfrp2, etc.) were also included.

Table S1. KEGG pathways enriched by 377 DEGs up-regulated in T5R1 and T10R1 groups (study I)

KEGG ID	KEGG pathway	FDR
mmu:04512	ECM–receptor interaction	3.45E-08
mmu:04510	Focal adhesion	7.89E-07
mmu:04974	Protein digestion and absorption	1.11E-06
mmu:04110	Cell cycle	6.95E-05

Table S2. GO terms enriched by 377 DEGs up-regulated in T5R1 and T10R1 groups (study I)

GO ID	GO biological process term	FDR
GO:0007049	Cell cycle	9.95E-07
GO:0030199	Collagen fibril organization	1.31E-06
GO:0051301	Cell division	4.39E-06
GO:0007155	Cell adhesion	6.65E-05
GO:0007067	Mitosis	1.10E-04
GO:0018149	Peptide cross-linking	1.84E-03
GO:0006898	Receptor-mediated endocytosis	2.30E-03
GO:0030198	ECM organization	4.58E-03
GO:0006935	Chemotaxis	5.69E-03
GO:0006270	DNA-dependent DNA replication initiation	6.40E-03
GO:0006334	Nucleosome assembly	8.35E-03
GO:0030335	Positive regulation of cell migration	9.09E-03
GO:0060346	Bone trabecula formation	2.50E-02
GO:0008285	Negative regulation of cell proliferation	4.19E-02
GO:0008284	Positive regulation of cell proliferation	5.02E-02
GO:0016525	Negative regulation of angiogenesis	5.84E-02
GO:0001525	Angiogenesis	7.29E-02
GO:0045766	Positive regulation of angiogenesis	9.79E-02

Table S3. KEGG pathway enriched by 422 up-regulated DEGs over T1R1, T2R1, and T3R1 groups (study II)

KEGG ID	KEGG pathway	FDR
mmu:04512	ECM–receptor interaction	1.37E-09
mmu:04145	Phagosome	6.00E-08
mmu:04510	Focal adhesion	2.65E-06
mmu:04974	Protein digestion and absorption	1.88E-04
mmu:04110	Cell cycle	1.51E-03
mmu:04666	Fc-γ R-mediated phagocytosis	8.11E-03
mmu:04380	Osteoclast differentiation	1.46E-02
mmu:03030	DNA replication	7.59E-02
mmu:04062	Chemokine signaling pathway	9.87E-02

Table S4. GO terms enriched by 422 up-regulated DEGs over T1R1, T2R1, and T3R1 groups (study II)

GO ID	GO biological process term	FDR
GO:0007049	Cell cycle	3.39E-09
GO:0030199	Collagen fibril organization	3.45E-09
GO:0030335	Positive regulation of cell migration	6.54E-09
GO:0007155	Cell adhesion	1.53E-07
GO:0051301	Cell division	1.59E-06
GO:0007229	Integrin-mediated signaling pathway	1.60E-06
GO:0007067	Mitosis	1.94E-05
GO:0051258	Protein polymerization	5.62E-05
GO:0006260	DNA replication	6.86E-05
GO:0007017	Microtubule-based process	4.51E-04
GO:0010811	Positive regulation of cell substrate adhesion	4.51E-04
GO:0007018	Microtubule-based movement	1.16E-03
GO:0001525	Angiogenesis	1.59E-03
GO:0042590	Antigen processing and presentation of exogenous peptide antigen by MHC class I	3.08E-03
GO:0030593	Neutrophil chemotaxis	3.23E-03
GO:0006954	Inflammatory response	3.84E-03
GO:0043066	Negative regulation of apoptotic process	4.15E-03
GO:0045576	Mast cell activation	4.41E-03
GO:0070208	Protein heterotrimerization	4.41E-03
GO:0016525	Negative regulation of angiogenesis	1.16E-02
GO:0006270	DNA-dependent DNA replication initiation	1.19E-02
GO:0006935	Chemotaxis	1.78E-02
GO:0007160	Cell matrix adhesion	2.15E-02
GO:0050870	Positive regulation of T-cell activation	2.71E-02
GO:0045766	Positive regulation of angiogenesis	2.90E-02
GO:0000910	Cytokinesis	3.29E-02
GO:0001805	Positive regulation of type III hypersensitivity	3.75E-02
GO:0002246	Wound healing involved in inflammatory response	3.75E-02
GO:0001568	Blood vessel development	4.92E-02
GO:0018149	Peptide cross-linking	9.93E-02

Table S5. GO terms enriched by DEGs common between study I and study II, study I-specific DEGs, and study II-specific DEGs at the enrichment *P* value less than 0.001

GO ID	GO terms	Common	Study II (T1R1–T3R1)	Study I (T5R1–T10R1)	Biological function
GO:0007049	Cell cycle	12.7189	1.8910	0.3773	
GO:0051301	Cell division	10.9377	1.0369	0.5714	
GO:0007067	Mitosis	9.4053	1.0494	0.0000	
GO:0000910	Cytokinesis	5.9324	0.0000	0.0000	Cell cycle, cell proliferation
GO:0006270	DNA-dependent DNA replication initiation	5.4371	0.0000	0.0000	
GO:0030308	Negative regulation of cell growth	4.3354	1.2248	0.0000	
GO:0008284	Positive regulation of cell proliferation	3.5597	1.5807	2.1988	
GO:0051726	Regulation of cell cycle	3.0640	1.4918	0.0000	
GO:0050870	Positive regulation of T-cell activation	5.1621	0.0000	0.0000	
GO:0050777	Negative regulation of immune response	4.4611	0.0000	0.0000	
GO:0071230	Cellular response to amino acid stimulus	4.2600	0.0000	0.0000	
GO:0002244	Hemopoietic progenitor cell differentiation	4.0001	0.0000	0.0000	
GO:0006935	Chemotaxis	3.9321	2.2347	2.6723	Immune system response, response to stimulus
GO:0019886	Antigen processing and presentation of exogenous peptide antigen by MHC class II	3.6649	0.0000	0.0000	
GO:0071356	Cellular response to TNF	3.6649	0.0000	0.0000	
GO:0045648	Positive regulation of erythrocyte differentiation	3.4833	0.0000	0.0000	
GO:0043029	T-cell homeostasis	3.2535	0.0000	0.0000	
GO:0034097	Response to cytokine stimulus	3.0710	0.0000	0.0000	
GO:0030199	Collagen fibril organization	10.1360	2.8250	0.0000	
GO:0018149	Peptide cross-linking	6.3137	0.0000	0.0000	
GO:0070208	Protein heterotrimerization	5.7670	0.0000	0.0000	
GO:0016525	Negative regulation of angiogenesis	5.3990	0.0000	0.0000	
GO:0043066	Negative regulation of apoptotic process	4.9379	2.1041	0.4434	
GO:0001568	Blood vessel development	4.9221	0.0000	0.0000	
GO:0032964	Collagen biosynthetic process	4.9027	0.0000	0.0000	
GO:0045600	Positive regulation of fat cell differentiation	4.6267	0.0000	0.0000	
GO:0033630	Positive regulation of cell adhesion mediated by integrin	4.4611	0.0000	0.0000	
GO:0007399	Nervous system development	4.4439	0.0000	0.0000	Development, differentiation, cytoskeleton organization etc.
GO:0043588	Skin development	4.3246	0.0000	0.0000	
GO:0006334	Nucleosome assembly	4.0250	0.0000	2.3732	
GO:0030324	Lung development	3.7238	1.3593	0.0000	
GO:0043154	Negative regulation of cysteine-type endopeptidase activity involved in apoptotic process	3.6992	0.0000	0.0000	
GO:0030336	Negative regulation of cell migration	3.6023	0.0000	0.0000	
GO:0030036	Actin cytoskeleton organization	3.4899	0.0000	0.0000	
GO:0045671	Negative regulation of osteoclast differentiation	3.4018	0.0000	0.0000	
GO:0008584	Male gonad development	3.0710	0.0000	0.0000	
GO:0001501	Skeletal system development	3.0640	1.4918	0.0000	
GO:0051017	Actin filament bundle assembly	3.0027	0.0000	0.0000	
GO:0007155	Cell adhesion	5.4843	5.8304	3.2059	
GO:0030335	Positive regulation of cell migration	5.1357	7.4461	1.4692	
GO:0006260	DNA replication	4.1869	4.3542	0.0000	
GO:0001525	Angiogenesis	3.9178	3.3020	1.6804	
GO:0010811	Positive regulation of cell substrate adhesion	3.7383	3.8398	0.0000	
GO:0007229	Integrin-mediated signaling pathway	3.3947	6.8947	0.0000	

Table S5. Cont.

GO ID	GO terms	Common	Study II (T1R1–T3R1)	Study I (T5R1–T10R1)	Biological function
GO:0002246	Wound healing involved in inflammatory response	0.0000	6.2752	0.0000	
GO:0045576	Mast cell activation	0.0000	4.0786	0.0000	
GO:0030593	Neutrophil chemotaxis	2.7047	4.0650	0.0000	
GO:0050729	Positive regulation of inflammatory response	0.0000	4.0650	0.0000	
GO:0006954	Inflammatory response	2.9719	3.8956	2.2704	
GO:0050766	Positive regulation of phagocytosis	0.0000	3.8398	0.0000	
GO:0050829	Defense response to Gram-negative bacterium	0.0000	3.2626	0.0000	
GO:0009617	Response to bacterium	0.0000	3.0791	0.0000	
GO:0051258	Protein polymerization	0.0000	8.9128	0.0000	
GO:0007017	Microtubule-based process	0.0000	8.1212	0.0000	
GO:0007018	Microtubule-based movement	1.7081	5.9588	0.0000	
GO:0006184	GTP catabolic process	0.0000	4.8403	0.0000	
GO:0045766	Positive regulation of angiogenesis	2.4302	3.4880	2.9724	
GO:0007159	Leukocyte cell–cell adhesion	0.0000	3.2626	0.0000	
GO:0007160	Cell matrix adhesion	2.9422	3.0402	0.0000	
GO:0030198	ECM organization	3.0410	1.4789	3.7224	
GO:0008285	Negative regulation of cell proliferation	1.9339	0.3942	4.1969	
GO:0006898	Receptor-mediated endocytosis	3.1838	0.0000	3.8706	

The numeric value denotes $-\log_{10}$ (P value), and the color represents the enrichment significance [from $P = 0.001$ (white) to $P = 1.0 \times 10^{-7}$ (red)].

Table S6. KEGG pathways enriched by 76 DEGs, a subset of 713 DEGs that was significantly affected by miR-29 transfection study (changed greater than ±1.5-fold)

KEGG ID	KEGG pathway	FDR
mmu:04512	ECM–receptor interaction	6.82E-10
mmu:04974	Protein digestion and absorption	1.06E-08
mmu:04510	Focal adhesion	3.08E-06

Table S7. GO terms enriched by 76 DEGs, a subset of 713 DEGs that was significantly affected by miR-29 transfection study (changed greater than ±1.5-fold)

GO ID	GO biological process term	FDR
GO:0030199	Collagen fibril organization	1.92E-06
GO:0070208	Protein heterotrimerization	2.11E-04
GO:0071230	Cellular response to amino acid stimulus	4.24E-04
GO:0001501	Skeletal system development	1.94E-03
GO:0032964	Collagen biosynthetic process	4.39E-03
GO:0001568	Blood vessel development	8.29E-03
GO:0016477	Cell migration	1.35E-02
GO:0043588	Skin development	9.62E-02